





# The Drying Kinetics of Arctium Lappa Roots in a Combined Infrared–Vacuum Dryer: An Experiment

Minh Ha Nguyen<sup>1</sup>, Luan Nguyen Thanh<sup>2\*</sup>

<sup>1</sup> Division of Mechanical Engineering, Campus in Ho Chi Minh City, University of Transport and Communications, Ho Chi Minh City 700000, Vietnam

<sup>2</sup> Faculty of Vehicle and Energy Engineering, Ho Chi Minh City University of Technology and Education (HCMUTE), Ho Chi Minh City 700000, Vietnam

Corresponding Author Email: [luannt@hcmute.edu.vn](mailto:luannt@hcmute.edu.vn)

Copyright: ©2025 The authors. This article is published by IETA and is licensed under the CC BY 4.0 license (<http://creativecommons.org/licenses/by/4.0/>).

<https://doi.org/10.18280/ijht.430416>

## ABSTRACT

**Received:** 2 June 2025

**Revised:** 25 July 2025

**Accepted:** 4 August 2025

**Available online:** 31 August 2025

### Keywords:

*infrared–vacuum dryer, Arctium lappa, drying kinetics*

This study aims to determine the drying kinetics of Arctium lappa roots in a combined infrared–vacuum dryer. The effects of 45–65°C drying temperatures and 6–24 kPa system pressures on the drying kinetics were considered. The results indicated that the sample dried faster as the drying temperature increased and the system pressure decreased. At a 6 kPa system pressure, the drying time was reduced by up to 23.8% and 46.7% compared to drying at 15 kPa and 24 kPa system pressures, respectively. In a drying regime with 45–65°C drying temperatures and 6 kPa system pressure, the mathematical model in the form of a third-order polynomial yielded the best prediction of the moisture content reduction. The effective moisture diffusivity coefficient was  $1.80 \times 10^{-10} - 3.56 \times 10^{-10} \text{ m}^2/\text{s}$ . The results provide valuable data regarding the theoretical and practical aspects of drying Arctium lappa roots in a combined infrared–vacuum dryer.

## 1. INTRODUCTION

Infrared radiation has the advantages of fast heating, low energy consumption, and bactericidal ability [1, 2]. Therefore, combining infrared radiation with other drying technologies has been considered. Studies on infrared-assisted convective drying [3-5], infrared-assisted heat pump drying [6, 7], combined infrared–vacuum drying [8-10], and infrared-assisted freeze drying [11-14] indicated that combining infrared radiation offered significant benefits regarding the efficiency and quality of dried products. Combined infrared–vacuum drying has the potential to yield high-quality dried products. Under the influence of infrared radiation and a vacuum environment, a low drying temperature ensures an appropriate drying time, and the vacuum environment limits material oxidation in the drying process. Therefore, combined infrared–vacuum is a potential drying method for temperature-sensitive materials. Recently, researchers have conducted drying kinetics studies for many different materials, such as mushroom [8], pumpkin [9], kiwifruit [10], lemon [15], grapefruit [16], banana bract powder [17], Cistanche [18], and potato [19]. The reports provide valuable data related to drying in a combined infrared–vacuum dryer.

Arctium lappa (ARL) is a herb of the Asteraceae family commonly grown in Asian countries. It can be used to treat colds, edema, and anti-inflammatory. ARL is often harvested seasonally; so, drying is a simple way to prolong its shelf life. The simplest drying method is sun-drying; however, it is

dependent on the weather and can accumulate dust. Thus, artificial drying has been preferentially applied. Nguyen et al. [20] studied the drying kinetics of ARL roots in a hot air dryer. Xia et al. [21] examined the color and flavor substances of ARL roots using different drying methods. The flavor composition of dried ARL roots was also analyzed in the report of Lu et al. [22]. Our review of the literature indicated that while the drying characteristics of ARL have been considered in a few studies, to our knowledge, data on the mathematical model and effective moisture diffusivity coefficient have not been provided. These data are important in predicting drying times for design and operation. Therefore, this research gap is addressed in the present work. The results provide a useful reference for drying ARL roots in a combined infrared–vacuum dryer.

## 2. ANALYTICAL METHODS

### 2.1 Materials

Fresh samples after harvest were selected and stored in vacuum-sealed bags at 5°C. The samples were sliced into elliptical shapes with dimensions of  $(45 \pm 5 \text{ mm}) \times (20 \pm 3 \text{ mm})$ , and each slice was  $4 \pm 0.2 \text{ mm}$  thick. The initial moisture content of ARL was determined by the oven drying method [23]. It was approximately 0.78 w.b, with an uncertainty of less than 0.2%.

## 2.2 Experimental description

Figure 1 shows the combined infrared–vacuum dryer used in this study. In the dryer, an infrared radiation lamp was placed 20 cm from the surface of the drying tray; the tray was 38 cm × 38 cm in size and had a digital scale beneath with an accuracy of 0.01 g to obtain the parameters during testing. A temperature sensor was used to monitor the temperature in the drying chamber (resolution of 0.1°C), and a digital vacuum pressure gauge was used to measure the system pressure (resolution of 0.1 kPa). The material arrangement density was approximately 2.43 kg/m<sup>2</sup>. Each experiment was replicated three times, and the values were averaged. Data were collected every ten minutes. The process was conducted from the initial moisture content to a final moisture of 10% w.b.

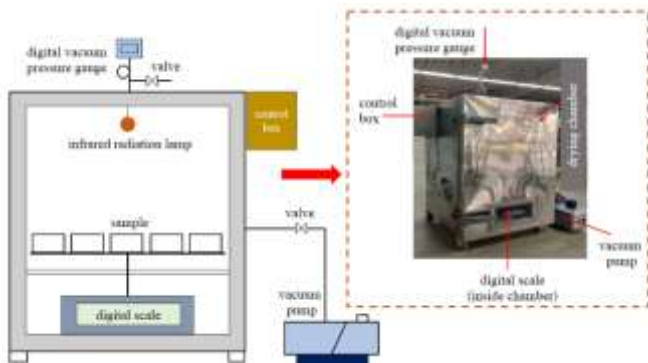


**Figure 1.** The combined infrared–vacuum dryer

## 2.3 Analysis of the drying kinetics

The drying kinetics were interpreted based on the computed results of the dry basis moisture content and moisture ratio. The dry basis moisture content was calculated according to the following formula:

$$M_i = \frac{G_i - G_s}{G_s} \quad (1)$$

Ignoring the equilibrium moisture content, the moisture ratio was calculated using the following formula [24]:

$$Y = \frac{M_i}{M_o} \quad (2)$$

In this work, six mathematical models were applied for kinetics modeling of ARL roots drying in a combined infrared–vacuum dryer [23, 25]:

- 1/ Henderson and Pabis:  $Y = a \cdot \exp(-kt)$ ;
- 2/ Page:  $Y = \exp(-kt^n)$ ;
- 3/ Logarithmic:  $Y = a \cdot \exp(-kt) + b$ ;
- 4/ Newton:  $Y = \exp(-kt)$ ;
- 5/ Wang and Singh:  $Y = 1 + at + bt^2$ ;
- 6/ Third-order polynomial:  $Y = 1 + at + bt^2 + ct^3$ .

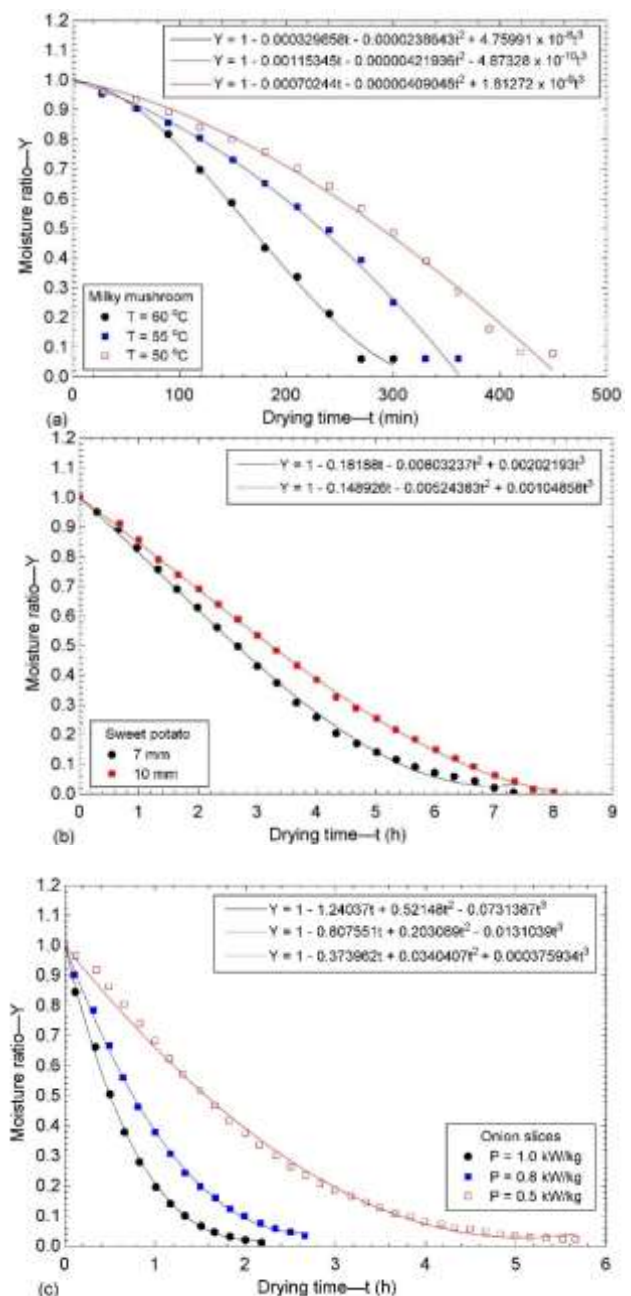
The present work used statistical parameters (correlation coefficient:  $R^2$ , root mean square error: RMSE, and reduced chi-squared:  $C_r^2$ ) to select the best-fitting model. The best-fitting model had the highest  $R^2$ , the lowest RMSE, and the lowest  $C_r^2$ . The statistical parameters were determined using the following formulas [23, 26, 27]:

$$R^2 = 1 - \frac{\sum_{i=1}^N (Y_{e,i} - Y_{p,i})^2}{\sum_{i=1}^N (Y_{e,m} - Y_{e,i})^2} \quad (3)$$

$$RMSE = \sqrt{\frac{1}{N} \sum_{i=1}^N (Y_{p,i} - Y_{e,i})^2} \quad (4)$$

$$C_r^2 = \frac{1}{N - z} \sum_{i=1}^N (Y_{p,i} - Y_{e,i})^2 \quad (5)$$

A model in the form of a third-order polynomial is proposed, based on the Wang and Singh model [28]. Drying data of several materials were used to evaluate the potential use of the third-order model. The results show that the third-order polynomial model fits the data points well (see Figure 2). Therefore, this model can be applied in drying kinetics studies.



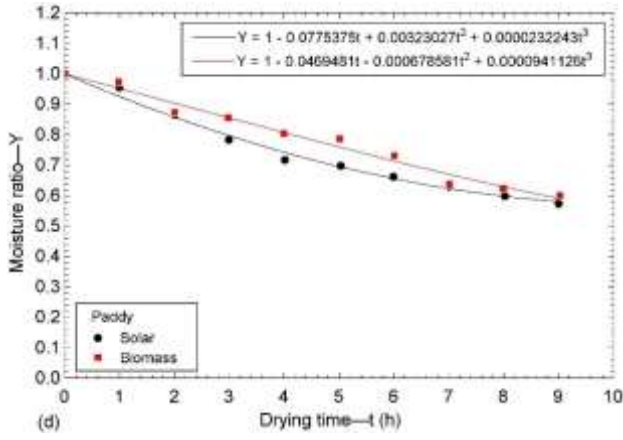


**Figure 2.** The potential of using the third-order polynomial model: (a) milky mushroom [29]; (b) sweet potato [30]; (c) onion [31]; (d) paddy [27]

The effective moisture diffusivity coefficient ( $D_{eff}$ ) is an important parameter in the modeling of the drying process. According to Fick's second law of diffusion, the differential equation for moisture diffusion is as follows:

$$\frac{\partial M}{\partial t} = D_{eff} \nabla^2 M \quad (6)$$

We assumed the initial moisture was uniformly distributed, with constant diffusion, dismissible shrinkage, and dismissible external resistance, and the material was a slab geometry. The approximate analytical solution for Eq. (6) is [16, 32]:

$$Y = \frac{M_i - M_e}{M_o - M_e} = \frac{8}{\pi^2} \sum_{n=0}^{\infty} \frac{1}{(2n+1)^2} \exp\left(-\frac{(2n+1)^2 \pi^2 D_{eff} t}{4L^2}\right) \quad (7)$$

Assuming a long drying time and ignoring the equilibrium moisture content, the approximation of Eq. (7) has the following form [10, 16]:

$$Y = \frac{M_i}{M_o} = \frac{8}{\pi^2} \exp\left(-\frac{\pi^2 D_{eff} t}{4L^2}\right) \quad (8)$$

Eq. (8) can further be simplified in logarithmic form:

$$\ln Y = \ln\left(\frac{8}{\pi^2}\right) - \frac{\pi^2 D_{eff} t}{4L^2} \quad (9)$$

The slope of the function  $\ln(Y)$  with the variable ( $t$ ) is the basis for determining the  $D_{eff}$ .

The standard deviation of the computed results was determined using the following formula [33]:

$$s = \sqrt{\frac{1}{(n-1)} \sum_{j=1}^n (x_j - x_m)^2} \quad (10)$$

The uncertainty of the calculated results was determined using the following formula [34]:

$$U_F = \left( \sum_{j=1}^n \left[ \left( \frac{\partial F}{\partial X_j} \right)^2 (U_{X_j})^2 \right] \right)^{0.5} \quad (11)$$

### 3. RESULTS AND DISCUSSION

Figure 3 shows the effect of the drying temperature and system pressure on the drying time. Under constant system pressure conditions, the drying time at 65°C was reduced by 25.0–35.4% and 45.8–65.6% compared to 55°C and 45°C, respectively. When observed under constant temperature conditions, the drying time at 6 kPa system pressure was reduced by 12.5–23.8% and 16.1–46.7% compared to drying at 15 kPa and 24 kPa system pressures, respectively. The water molecules receive more energy as the drying temperature increases, increasing moisture diffusion from the center to the shell. Furthermore, there is a high difference in vapor pressure between the material surface and the environment in the drying chamber, leading to increased water escape from the material surface. Thus, the drying time decreased as the drying temperature increased and the system pressure decreased. Drying at a low system pressure was suitable for a reasonable drying time. Therefore, in the next part of the study, the drying kinetics were examined in detail at 6 kPa system pressure and 45–65°C drying temperatures.

Figure 4(a) shows the data points of the three drying regimes. The six mathematical models were applied to determine the best-fitting mathematical model for the data points. The results in Table 1 indicate that the sixth mathematical model best described the drying characteristics of ARL roots due to the highest  $R^2$ , the lowest RMSE, and the lowest  $C_r^2$ . The coefficients in the third-order polynomial model are detailed in Table 2. Figure 4(b) confirms a good fit between the mathematical model in third-order polynomial form and the data points, with a high accuracy in prediction. Furthermore, this model is simple in form and advantageous for the practical application of predicting the moisture content variation with drying time. Therefore, this model should be considered for drying kinetics studies.

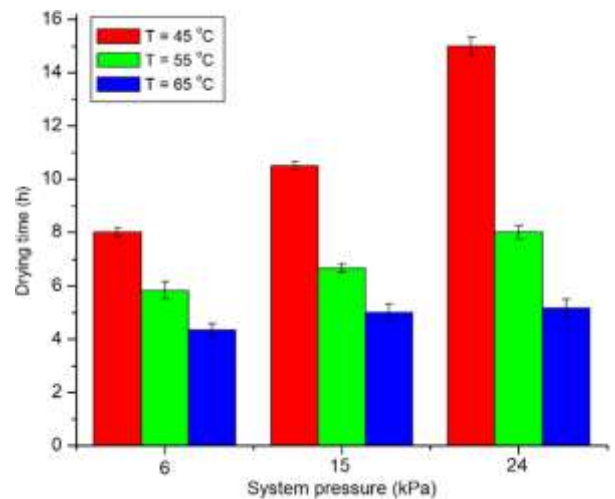


**Figure 3.** Effect of drying regimes on the drying time

The effective moisture diffusivity coefficient was calculated according to Eq (9). The result shows that the  $D_{eff}$  obtained was from  $1.80 \times 10^{-10}$  to  $3.56 \times 10^{-10}$  m<sup>2</sup>/s (see Table 3). This

result was consistent with the data from some materials provided in the previous studies [15, 16].

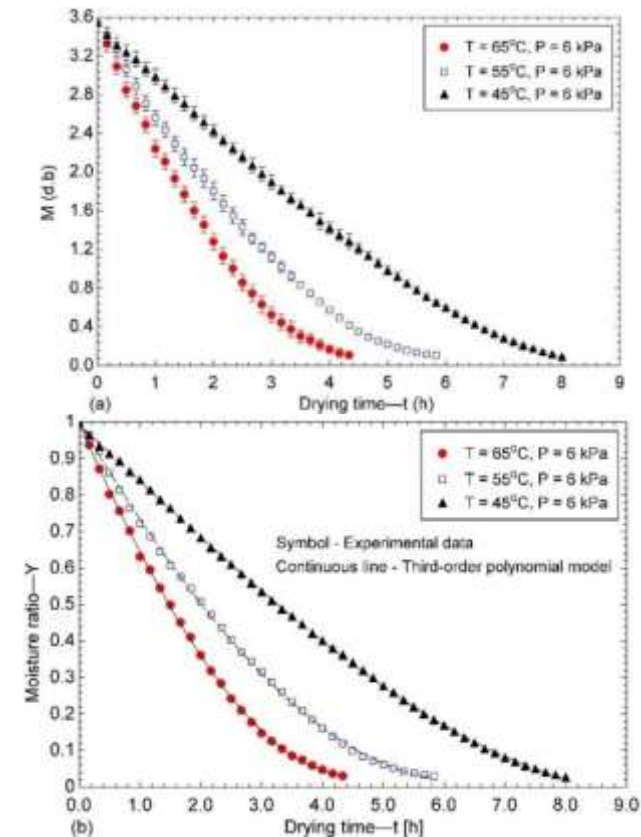


Figure 4. Experimental data and the regression: (a) experimental data; (b) predicted curve

Table 1. The statistical parameters of the mathematical models

Drying Mode	Model	Statistical Parameters		
		R <sup>2</sup>	RMSE	C <sub>r</sub> <sup>2</sup>
T=65°C, P=6 kPa	1	0.982766	0.042255	0.001928
	2	0.996437	0.018839	0.000383
	3	0.997930	0.013688	0.000211
	4	0.987456	0.049250	0.002519
	5	0.999492	0.006972	0.000052
	6	0.999730	0.005005	0.000028
T=55°C, P=6 kPa	1	0.981571	0.043610	0.002014
	2	0.995427	0.021106	0.000472
	3	0.998353	0.012186	0.000162
	4	0.987009	0.051833	0.002763
	5	0.999443	0.007431	0.000058
	6	0.999605	0.005970	0.000039
T=45°C, P=6 kPa	1	0.969571	0.054514	0.003098
	2	0.993582	0.025164	0.000660
	3	0.999016	0.009314	0.000092
	4	0.977323	0.063870	0.004164
	5	0.999391	0.007629	0.000061
	6	0.999881	0.003415	0.000012

Table 2. The coefficients in the third-order polynomial model

T (°C)	P (kPa)	Coefficients		
		a	b	c
65	6	-0.384026	0.0272412	0.00227276
55	6	-0.281214	0.0145357	0.000855446
45	6	-0.161599	0.000773081	0.00051556

Table 3. The D<sub>eff</sub> of ARL roots

T (°C)	P (kPa)	D <sub>eff</sub> (m <sup>2</sup> /s)
65	6	3.56 × 10 <sup>-10</sup>
55	6	2.72 × 10 <sup>-10</sup>
45	6	1.80 × 10 <sup>-10</sup>

4. CONCLUSIONS

The present work focused on determining the drying kinetics of ARL roots in a combined infrared–vacuum dryer. The drying regime was established with 45–65°C drying temperatures and 6–24 kPa system pressures. The main findings are as follows:

- 1) Increasing the drying temperature and decreasing the system pressure led to a faster drying process.
- 2) The third-order polynomial model best describes the drying characteristics of ARL roots in a combined infrared–vacuum dryer with a drying regime comprising 45–65°C drying temperatures and 6 kPa system pressure. This model can be used for studies related to drying kinetics.
- 3) In the drying mode with 45–65°C drying temperatures and 6 kPa system pressure, the effective moisture diffusivity coefficient of the dried samples was from 1.80 × 10<sup>-10</sup> to 3.56 × 10<sup>-10</sup> m<sup>2</sup>/s.
- 4) The present work investigated *Arctium lappa* roots' drying kinetics in a combined infrared–vacuum dryer. The results provide a useful direction for practice. Expanding the evaluation regarding energy consumption and optimization in future studies is necessary, as well as considering the color, vitamins, and trace elements in *Arctium lappa* roots to understand the quality obtained with the present method.

REFERENCES

[1] Delfiya, D.A., Prashob, K., Murali, S., Alfiya, P.V., Samuel, M.P., Pandiselvam, R. (2022). Drying kinetics of food materials in infrared radiation drying: A review. *Journal of Food Process Engineering*, 45(6): e13810. <https://doi.org/10.1111/jfpe.13810>

[2] Huang, D., Yang, P., Tang, X., Luo, L., Sunden, B. (2021). Application of infrared radiation in the drying of food products. *Trends in Food Science & Technology*, 110: 765-777. <https://doi.org/10.1016/j.tifs.2021.02.039>

[3] Wen, Y.X., Chen, L.Y., Li, B.S., Ruan, Z., Pan, Q. (2021). Effect of infrared radiation-hot air (IR-HA) drying on kinetics and quality changes of star anise (*Illicium verum*). *Drying Technology*, 39(1): 90-103. <https://doi.org/10.1080/07373937.2019.1696816>

[4] Onwude, D.I., Hashim, N., Abdan, K., Janius, R., Chen, G. (2019). The effectiveness of combined infrared and hot-air drying strategies for sweet potato. *Journal of Food Engineering*, 241: 75-87. <https://doi.org/10.1016/j.jfoodeng.2018.08.008>

[5] Xu, H., Wu, M., Wang, Y., Wei, W., Sun, D., Li, D., Gao, F. (2022). Effect of combined infrared and hot air drying strategies on the quality of Chrysanthemum (*Chrysanthemum morifolium* Ramat.) cakes: Drying behavior, aroma profiles and phenolic compounds. *Foods*, 11(15): 2240. <https://doi.org/10.3390/foods11152240>



- [6] Aktaş, M., Khanlari, A., Amini, A., Şevik, S. (2017). Performance analysis of heat pump and infrared–heat pump drying of grated carrot using energy-exergy methodology. *Energy Conversion and Management*, 132: 327-338. <https://doi.org/10.1016/j.enconman.2016.11.027>
- [7] Malçok, S.D., Karabacak, A.Ö., Bekar, E., Tunçkal, C., Tamer, C.E. (2023). Influence of a hybrid drying combined with infrared and heat pump dryer on drying characteristics, colour, thermal imaging and bioaccessibility of phenolics and antioxidant capacity of mushroom slices. *Journal of Agricultural Engineering*, 54(3): 1537. <https://doi.org/10.4081/jae.2023.1537>
- [8] Salehi, F., Kashaninejad, M., Jafarianlari, A. (2017). Drying kinetics and characteristics of combined infrared-vacuum drying of button mushroom slices. *Heat and Mass Transfer*, 53(5): 1751-1759. <https://doi.org/10.1007/s00231-016-1931-1>
- [9] Ghaboos, S.H.H., Ardabili, S.M.S., Kashaninejad, M., Asadi, G., Aalami, M. (2016). Combined infrared-vacuum drying of pumpkin slices. *Journal of Food Science and Technology*, 53(5): 2380-2388. <https://doi.org/10.1007/s13197-016-2212-1>
- [10] Aidani, E., Hadadkhodaparast, M., Kashaninejad, M. (2017). Experimental and modeling investigation of mass transfer during combined infrared-vacuum drying of Hayward kiwifruits. *Food Science & Nutrition*, 5(3): 596-601. <https://doi.org/10.1002/fsn3.435>
- [11] Oliveira, N.L., Alexandre, A.C.S., Silva, S.H., de Abreu Figueiredo, J., Rodrigues, A.A., de Resende, J.V. (2023). Drying efficiency and quality preservation of blackberries (*Rubus* spp. variety Tupy) in the near and mid-infrared-assisted freeze-drying. *Food Chemistry Advances*, 3: 100550. <https://doi.org/10.1016/j.focha.2023.100550>
- [12] Antal, T., Tarek-Tilistyyák, J., Cziáky, Z., Sinka, L. (2017). Comparison of drying and quality characteristics of pear (*Pyrus communis* L.) using mid-infrared-freeze drying and single stage of freeze drying. *International Journal of Food Engineering*, 13(4): 20160294. <https://doi.org/10.1515/ijfe-2016-0294>
- [13] Khampakool, A., Soisungwan, S., Park, S.H. (2019). Potential application of infrared assisted freeze drying (IRAFD) for banana snacks: Drying kinetics, energy consumption, and texture. *LWT*, 99: 355-363. <https://doi.org/10.1016/j.lwt.2018.09.081>
- [14] Oliveira, N.L., Silva, S.H., de Abreu Figueiredo, J., Norcino, L.B., de Resende, J.V. (2021). Infrared-assisted freeze-drying (IRFD) of açai puree: Effects on the drying kinetics, microstructure and bioactive compounds. *Innovative Food Science & Emerging Technologies*, 74: 102843. <https://doi.org/10.1016/j.ifset.2021.102843>
- [15] Salehi, F., Kashaninejad, M. (2018). Modeling of moisture loss kinetics and color changes in the surface of lemon slice during the combined infrared-vacuum drying. *Information processing in Agriculture*, 5(4): 516-523. <https://doi.org/10.1016/j.inpa.2018.05.006>
- [16] Salehi, F., Kashaninejad, M. (2018). Mass transfer and color changes kinetics of infrared-vacuum drying of grapefruit slices. *International Journal of Fruit Science*, 18(4): 394-409. <https://doi.org/10.1080/15538362.2018.1458266>
- [17] Chittrakorn, S., Ruttarattanamongkol, K., Detyothin, S., Kongbangkerd, T. (2024). Effect of vacuum infrared drying and tray drying on physicochemical properties, antioxidant activities, and  $\alpha$ -amylase and  $\alpha$ -glucosidase inhibition of banana bract powder. *International Food Research Journal*, 31(5): 1155-1164. <https://doi.org/10.47836/ifrj.31.5.07>
- [18] Jiang, C., Wan, F., Zang, Z., Zhang, Q., Xu, Y., Huang, X. (2022). Influence of far-infrared vacuum drying on drying kinetics and quality characteristics of Cistanche slices. *Journal of Food Processing and Preservation*, 46(12): e17144. <https://doi.org/10.1111/jfpp.17144>
- [19] Mitrevski, V., Dedinac, A., Mitrevska, C. (2021). Estimation of thermophysical properties of far infrared vacuum drying potato by application of inverse approach. *Thermal Science*, 25(1 Part B): 603-611. <https://doi.org/10.2298/TSCI200415225M>
- [20] Nguyen, L.T., Nguyen, M.H., Le, H.S.N. (2023). Thin-layer drying of burdock root in a convective dryer: drying kinetics and numerical simulation. *Journal of Advanced Research in Fluid Mechanics and Thermal Sciences*, 104(1): 21-36. <https://doi.org/10.37934/arfmts.104.1.2136>
- [21] Xia, J., Guo, Z., Fang, S., Gu, J., Liang, X. (2021). Effect of drying methods on volatile compounds of burdock (*Arctium lappa* L.) root tea as revealed by gas chromatography mass spectrometry-based metabolomics. *Foods*, 10(4): 868. <https://doi.org/10.3390/foods10040868>
- [22] Lu, Y., Zhang, M., Sun, J., Cheng, X., Adhikari, B. (2014). Drying of burdock root cubes using a microwave-assisted pulsed spouted bed dryer and quality evaluation of the dried cubes. *Drying Technology*, 32(15): 1785-1790. <https://doi.org/10.1080/07373937.2014.945180>
- [23] Thanh, L.N., Minh, H.N., Le, H.S.N., Hoai, N.L. (2023). Thin-layer drying kinetics of pseudapocryptes elongatus fish in a convective dryer. *Journal of Advanced Research in Fluid Mechanics and Thermal Sciences*, 108(1): 158-172. <https://doi.org/10.37934/arfmts.108.1.158172>
- [24] Thanh, L.N. (2024). The mass transfer coefficient of pseudapocryptes elongatus fish dried in a hot air dryer. *International Journal of Heat & Technology*, 42(6): 158-172. <https://doi.org/10.18280/ijht.420617>
- [25] Adekanye, T., Alhassan, E., Amodu, M., Olanrewaju, T., Iyanda, M. (2025). Kinetics of heat and mass transfer in moringa leaves drying in a cabinet dryer. *Results in Engineering*, 26: 104763. <https://doi.org/10.1016/j.rineng.2025.104763>
- [26] Kong, L., Yang, X., Hou, Z., Dong, J. (2020). Mathematical modeling of drying kinetics for pulp sheet based on Fick's second law of diffusion. *Journal of Korea TAPPI*, 52(2): 23-31. <https://doi.org/10.7584/JKTAPPI.2020.04.52.2.23>
- [27] Manikantan, M.R., Barnwal, P., Goyal, R.K. (2014). Drying characteristics of paddy in an integrated dryer. *Journal of Food Science and Technology*, 51(4): 813-819. <https://doi.org/10.1007/s13197-013-1250-1>
- [28] Wang, C.Y., Singh, R.P. (1978). Use of variable equilibrium moisture content in modeling rice drying. *Transactions of American Society of Agricultural Engineers*, 11(6): 668-672.
- [29] Arumuganathan, T., Manikantan, M.R., Rai, R.D., Anandakumar, S., Khare, V. (2009). Mathematical modelling of drying kinetics of milky mushroom in a bed dryer. *International Agrophysics*, 23(1): 1-7.

- [30] Meng, Y., Wang, J., Fang, S., Chen, J. (2011). Drying characteristics and mathematical modeling of hot air drying of cooked sweet potatoes. Transactions of the Chinese Society of Agricultural Engineering, 27(7): 387-392.
- [31] Wang, J. (2002). A single-layer model for far-infrared radiation drying of onion slices. Drying Technology, 20(10): 1941-1953. <https://doi.org/10.1081/DRT-120015577>
- [32] Crank, J. (1979). The Mathematics of Diffusion. Oxford University Press. New York.
- [33] Lee, D.K., In, J., Lee, S. (2015). Standard deviation and standard error of the mean. Korean Journal of Anesthesiology, 68(3): 220-223. <https://doi.org/10.4097/kjae.2015.68.3.220>
- [34] Moffat, R.J. (1988). Describing the uncertainties in experimental results. Experimental Thermal and Fluid Science, 1(1): 3-17. [https://doi.org/10.1016/0894-1777\(88\)90043-X](https://doi.org/10.1016/0894-1777(88)90043-X)

## NOMENCLATURE

$G_i$	weight of the sample at time $i$ , g
$G_s$	weight of dry solids, g
$M$	dry basis moisture content
$Y$	moisture ratio

$t$	drying time, s
$L$	half thickness of slab, m
$D_{\text{eff}}$	effective moisture diffusivity coefficient, $\text{m}^2.\text{s}^{-1}$
$R^2$	correlation coefficient
RMSE	root mean square error
$C_r^2$	reduced chi-squared
$s$	standard deviation
$k$	drying constant, $\text{h}^{-1}$
$T$	drying temperature, $^{\circ}\text{C}$
$P$	system pressure, kPa
$z$	number of constants
$N$	number of observations
$a, b, c$	coefficients
$U$	uncertainty
$\Delta$	difference

## Subscripts

$o$	initial
$i$	at time $i$
$m$	mean
$e$	equilibrium
$F$	calculated results
$X_j$	measured parameter
$e, i$	experimental value
$p, i$	predicted value